Monitoring of the mechanical behavior of concrete with chemically treated steel fibers by acoustic emission

D.G. Aggelis [a,*], D.V. Soulioti [b], E.A. Gatselou [b], N.-M. Barkoula [b], T.E. Matikas [b]

[a] Department of Mechanics of Materials and Constructions, Vrije Universiteit Brussel, 1050 Brussels, Belgium
[b] Department of Materials Science and Engineering, University of Ioannina, 45110 Ioannina, Greece

HIGHLIGHTS

▶ Continuous monitoring of the differences in fracture mechanisms of surface treated and untreated fibers concrete.
▶ Monitoring of the differences in fracture mechanisms of concrete with different fiber shapes.
▶ Correlation of mechanical toughness with nondestructively tested parameters.

ARTICLE INFO

ABSTRACT

Inclusion of steel fibers is an effective way to increase the ductility of concrete. In order to achieve optimal mechanical properties and especially toughness, chemical treatment of the fibers is applied. Suitable agents improve the bonding between the stiff fiber and matrix enabling more efficient stress transfer. In the present study specimens with plain and chemically treated steel fibers are subjected to four-point bending with concurrent monitoring of their acoustic emission (AE) activity. Specific AE parameters demonstrate that coating offers distinct characteristics to the interphase especially after the maximum load has been reached. Parameters like average frequency (AF) and the rise angle of the waveforms, which are used for cracking mode classification, indicate that the post peak behavior of specimens with chemically treated fibers is more closely related to matrix cracking, while untreated exhibit clear shear behavior due to pull-out. It is concluded that coating effectively contributes to the deflection of the cracks from the fiber–matrix interphase into the concrete matrix. AE analysis sheds light into the fracturing behavior of concrete in real time, in a way that is not possible by any other conventional measurement.

© 2012 Elsevier Ltd. All rights reserved.

1. Introduction

Besides its low cost, easiness of forming and high compressive strength, concrete is characterized by relatively low toughness or capacity to absorb energy during fracture. One way to improve its brittle behavior is the inclusion of fibers. Fibers bridging the crack sides increase the resistance against crack opening by absorbing energy due to friction or other mechanisms [1,2]. Fibers have also been shown to improve tensile strength, durability in fatigue, surface resistance to wetting–drying cycles as well as to prevent concrete from cracking [3–7]. Steel fibers improve the bond between concrete and reinforcement in joints [8], while they improve the resistance to spalling [9] as well as the performance of concrete structures under torsional loads [10]. Steel fiber reinforced concrete (SFRC), similarly to other fiber reinforced materials, includes different fracture mechanisms. Specifically, concrete matrix cracking, detachment of aggregates and aggregate crushing which are also met in plain concrete [11], interfacial debonding of fibers [2], frictional fiber pull-out [12], fiber plastic deformation and possibly rupture of the fibers [11,12].

A key point for the performance of the materials is the quality of the bonding between the fibers and the matrix. Steel possesses considerably higher mechanical properties than concrete. However, in order to take full advantage of this potential, it is essential to achieve good quality bonding to lead to high stress transfer capacity [13]. In general, the more important mechanisms that promote stress transfer efficiency between concrete and steel are friction, mechanical interlocking (if the fibers are not straight) and surface treatment of the fibers either by chemical coating [14] or by other processes [15].

Acoustic emission (AE) enlightens the complicated processes within the material [16,17]. AE enables the monitoring of crack growth using transducers placed on the surface of the material. These sensors record the response after each cracking event and convert it into an electric waveform [18]. Information can be drawn about the location of the cracks and the cumulative activity,

while study of qualitative features leads to more detailed assessment of the fracture process [19]. Several AE features have been extensively studied in relation to the fracture process. One of them is the AE energy, which is the area under the rectified signal envelope. It is connected to the intensity of the cracking events [20]. Similarly the maximum amplitude of the waveforms depends on the cracking source, while frequency features like the "average frequency", AF, are indicative of the cracking mode. AF is the number of threshold crossings divided by the duration of each signal, measured in kHz. Another index studied in relation to the fracture mode is "RA value" which is the duration of the initial rising part of the waveform, over its maximum amplitude, in μs/V. The different types of failure processes, lead to wave emissions with distinct characteristics enabling the classification of cracks as to their mode [21]. Tensile cracks lead to emissions with higher frequency content as well as low RA values [22–24]. On the other hand shear types of failure such as delaminations, or fiber pull-out have been shown to produce signals with increased duration and RA and lower frequency in concrete or other materials [25,26].

Since different fracture mechanisms are activated, the AE characteristics are also shifting according to the dominant mode at each fracture stage. Several of the AE indices have been proposed to monitor changes in the microstructure due to damage accumulation. Specifically, RA has been shown to increase with damage, while AF decreases [27–29]. This has been proven in the case of four-point bending of SFRC, where at the initial stages of loading during micro-cracking AF remained at high levels while instantly after the major fracture incident, AF reduced by approximately 50–75%. RA inversely exhibited an explosive increase at the instance of fracture, remaining at high levels at the post-peak stage.

In this study, SFRC beams are tested in four-point bending with concurrent AE monitoring. Fibers were of different shapes, namely straight, hooked and undulated (wavy). AE was monitored during the fracture process for interpretation of the fracturing stage and fracture mode. Detailed study of specific parameters enables the assessment of the fracture process, which depends on the quality of the interface bonding. It is shown that the existence of chemical coating leaves a distinct fingerprint on the AE behavior especially after the initial matrix crack, when stresses are redistributed and the effect of reinforcement becomes evident. This study aims to help characterize the different damage mechanisms (matrix cracking and fiber pull-out) that occur successively or overlapping in SFRC and help in the tailoring of the properties of the constituent phases for improved behavior. This is the continuation of a study on the influence of chemical coating on the mechanical and AE behavior of SFRC [27,29] and is the first time that correlations between AE parameters and mechanical properties like toughness of SFRC with chemically coated fibers are presented.

2. Experimental details

2.1. Materials

Concrete specimens were produced in six mixtures of four specimens each. The maximum aggregate size was 10 mm and the water/cement ratio by mass was 0.50. The steel fibers were added in volume content of 1% and their tensile strength was 1100 MPa. The shapes used were straight with aspect ratio 63 and length 25 mm, undulated (wavy) with aspect ratio 43 and hooked with the same aspect ratio and length 30 mm. Half of the mixes (three) included plain (untreated) fibers and the other three treated for comparison. The chemical coating applied on the fibers was a zinc phosphate (ZnPh) conversion coating introduced by Sugama et al. [14]. The formulation for the coating liquid was 0.46 wt.% zinc orthophosphate dihydrate, 0.91 wt.% 85% H_3PO_4, and 98.63 wt.% water. The fibers were immersed in the conversion at 90 °C for 5 min and afterwards rinsed with water and dried for 10 min at 150 °C. For the four-point bending test, the ASTM C1609/C 1609M-05 was followed. Briefly, the size of the specimens was $100 \times 100 \times 400$ mm with bottom and top spans 300 mm and 100 mm respectively (Fig. 1). The experiment was terminated at the mid span deflection of 2 mm.
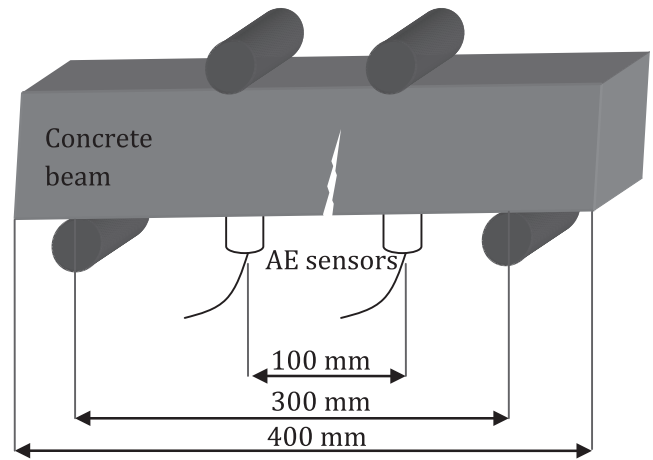

Fig. 1. Schematic representation of the four-point bending experimental setup and AE monitoring.

2.2. Acoustic emission measurements

Two AE sensors (Pico, PAC) were placed at the bottom side of the specimen (Fig. 1). In order to improve acoustic coupling roller bearing grease was applied between the sensors and the specimen's surface. The sensors were also secured by elastic tape in order to ensure their solid placement. The signals felt by the two sensors were transformed into electric waveforms and digitized in a two-channel monitoring board PCI-2 of PAC. The threshold and the pre-amplifier gain were set to 40 dB. The sampling rate was 5 MHz.

3. Results

As has been discussed in previous works, the AE activity of the four-point testing of SFRC beams can be divided in three stages [26], (see Fig. 2). The first is the initial micro-cracking stage (I), where load is continuously increasing. It is characterized by moderate acoustic emission due to minor cracks in the concrete matrix. The next is the macro-cracking stage (II) where the load drops and a macro-crack develops from the bottom tensile side towards the top. The rate of AE is high due to the number and high intensity
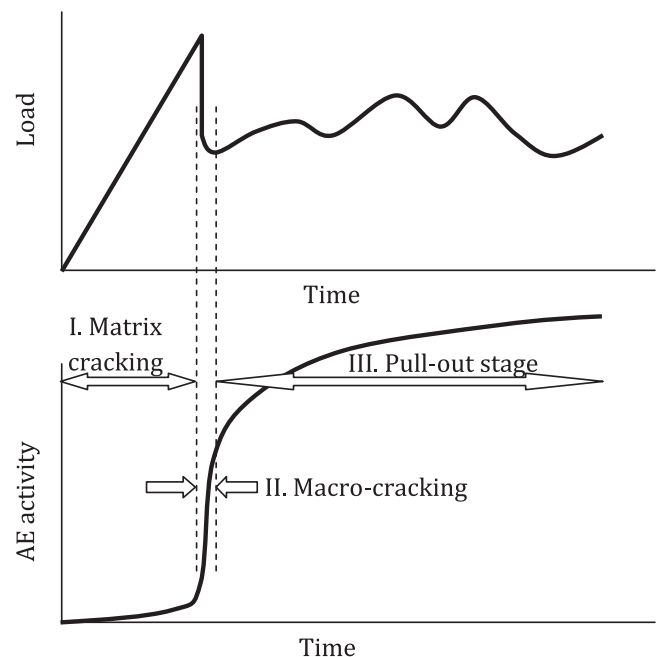

Fig. 2. Different stages in fracture test of SFRC with corresponding AE activity.
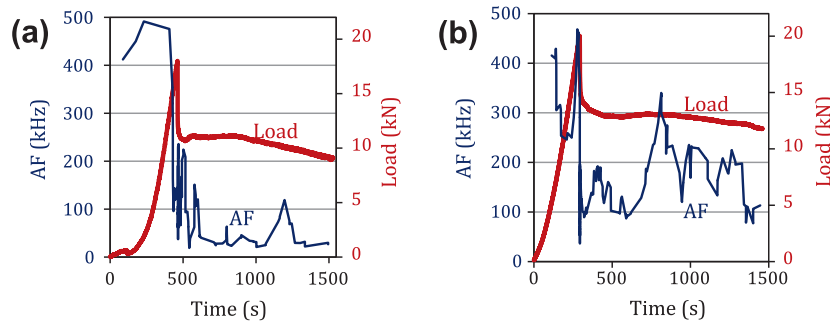
Fig. 3. Time histories of average frequency and load for specimens with straight fibers (a) untreated, (b) treated.
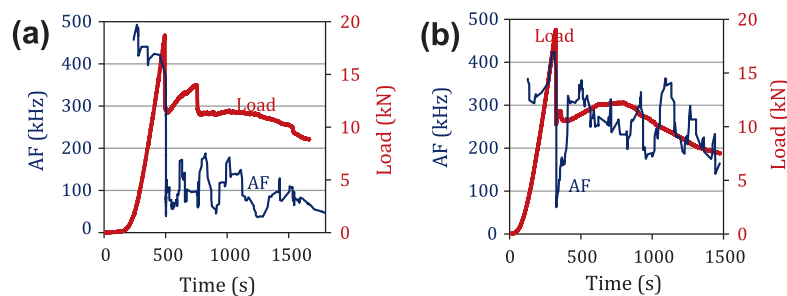

Fig. 4. Time histories of average frequency and load for specimens with undulated fibers (a) untreated, (b) treated.

of the cracking as well as the pull out of the fibers that are bridging the crack. This is the shortest stage. The last stage is dominated by the gradual pull out of fibers (III), while the cracking of the matrix continues. The AE rate in this stage gradually decelerates as the remaining number of fibers to be pulled out is decreasing continuously.

Fig. 3 shows the AF trend line (moving average of 50 points) along with the load history for two specimens with straight fibers; (a) with untreated and (b) with treated fibers. For both specimens AF lies near 400 kHz as the load is increasing. However, at the instance of macro-fracture (evident by the drop of load) AF severely decreases to values below 100 kHz. One distinct difference is that for the "treated fibers" specimen the AF line partially recovers towards the initial value (100 kHz to 300 kHz), while for the uncoated (Fig. 3a) the average value remains lower than 100 kHz.

Quite similar is the behavior of specimens with undulated fiber as can be seen in Fig. 4a and b. At stage I, before fracture both exhibit average value of AF around 400 kHz. Concerning the untreated fibers, at the instance of macro-fracturing, the values of the AF line strongly decrease and stay there during the whole pull out stage. As aforementioned, low AF corresponds to shearing mode of fracture. This is reasonable because after the load drop, pull-out becomes the active fracture mechanism. The friction between the fiber and the matrix resembles shear, and reasonably reduces the level of AF produced. For the treated fibers specimen (Fig. 4b), after the strong decrease at the main fracture instance, AF seems to fluctuate between 200 kHz and 300 kHz. This distinct AE behavior indicates the existence of differences in the fracturing behavior between treated and untreated fiber specimens as well. The frequency characteristics imply that along with the frictional pull-out events, matrix cracking continues since frequency lies in intermediate levels. This cracking occurs due to the deflection of the failure surface from the fiber–matrix interphase into the cementitious matrix, as a result of the good bonding of the fibers.

RA value also exhibits strong trends following fracture as well as distinct changes depending on the surface treatment. Fig. 5 shows the RA moving average of 50 hits along with the load for fibers with hooked ends in the absence of chemical coating (a)

and with chemical coating (b). In both load curves, there are two points of load drop, marked by arrows. At these instances, an explosive increase of RA is recorded which can be used as an indicator of high intensity damage events. For the uncoated fibers (Fig. 5a), RA continues to exhibit very strong fluctuations, reaching values near 4 or 5 ms/V. For the case of coated fibers (Fig. 5b) after instances of load drop, RA is usually restored at levels below or near 1 ms/V during most of the remaining fracture process. This implies that the fracture obtains characteristics of matrix cracking, which tend to lower the RA of the emitted AE signals compared to the ones of untreated fibers.

The above figures include comparisons of histories for indicative specimens, while the AE trends are repeatable in all specimens of each mixture. These distinct differences between coated and plain fiber specimens emerge at the post peak stage. This is reasonable since fibers start to seriously contribute to the fracture process, after the matrix has been ruptured. Therefore, at the post-peak stage it is more likely to monitor any differences due to fiber surface conditioning.

4. Correlation with mechanical parameters

4.1. Toughness

From the engineering point of view, the target of fiber reinforcement as well as fiber surface conditioning is the increase of toughness. Toughness is calculated as the area under the load–deflection curve until the deflection of 2 mm according to standard ASTM C1609/C1609M-05. Since chemical coating reinforces the bonding between the fibers and the matrix, in general the toughness of the specimens increases. This is evident for the straight fibers, the shape of which does not result in mechanical interlocking and the bond between fiber and matrix is the only mechanism that resists fracture after the matrix has been cracked at the post peak stage. The toughness of the specimens with treated straight fibers was approximately 40% increased compared to the corresponding untreated ones. The purpose of coating is to reinforce the
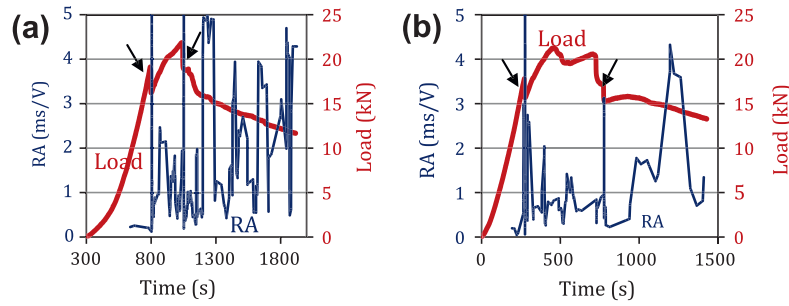
Fig. 5. Time histories of RA value and load for specimens with hooked fibers (a) untreated, (b) treated.
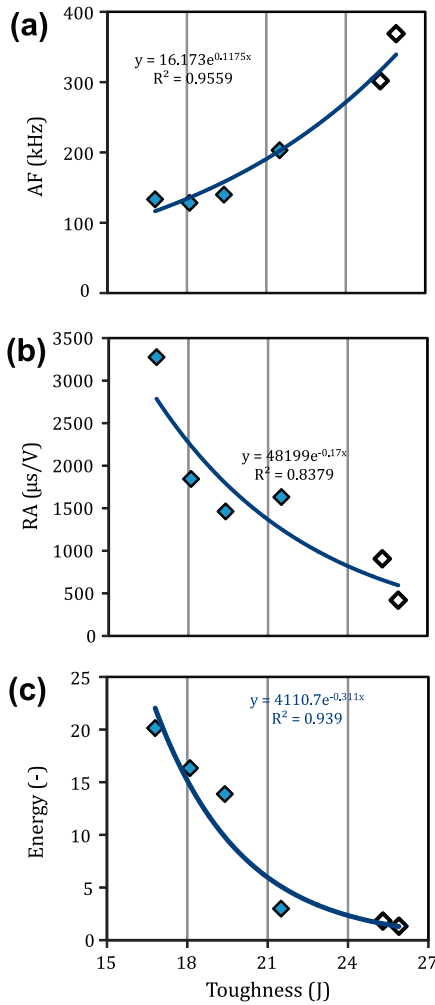

Fig. 6. Average frequency (a), RA value (b) and AE energy (c) of the post peak stage (III) vs. toughness for specimens with straight fibers. (Solid symbols denote untreated fibers, open denote treated).

Fig. 7. Average frequency during post-peak stage (III) (a), and total AE energy (b) vs. toughness and energy during macro-cracking stage (II) vs. peak load for seven mixes of concrete. (Solid symbols denote steel fiber concrete mixture, open symbol denotes plain concrete mixture).

interphase bonding so that fiber pull out requires more energy. If the bonding strength surpasses the matrix strength, small volumes of cement are detached from the matrix being firmly bonded on the fibers. This matrix cracking during pull out is an additional fracture mechanism, and therefore, it leaves its signature on the AE signals as demonstrated by the differences of the shifting trends of specific indices, like AF and RA, between treated and untreated fiber specimens. Since the actually measured toughness and the nature of the AE signals are firmly connected to the fracture mechanisms, correlations between them are reasonable to exist. Fig. 6a
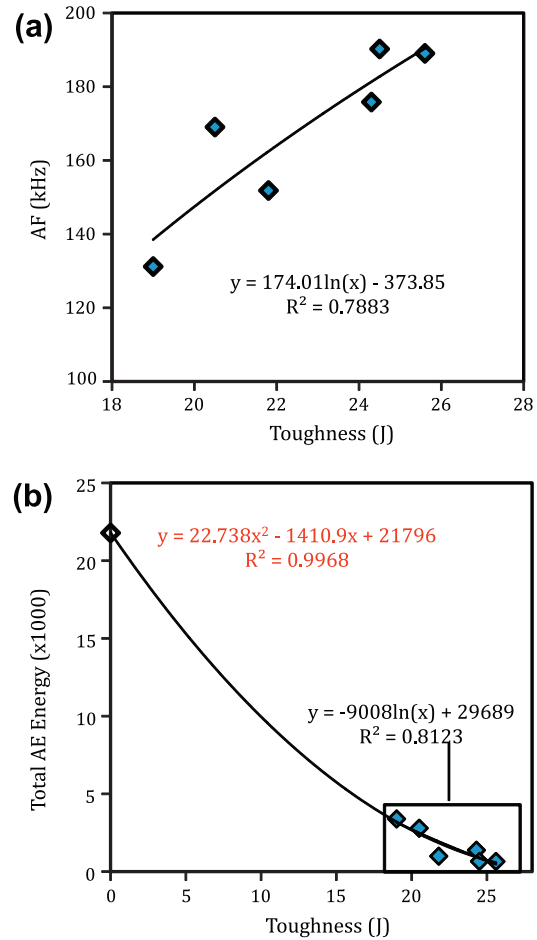
shows the average value of AF of the post peak stage (III, as in Fig. 2) vs. the measured toughness for six specimens with straight fibers appropriately tested in bending. The exponential fit exhibits a quite high correlation coefficient of 0.96. The positive correlation is evident for the four untreated specimens (solid symbols), and continues for the two treated, which absorb considerable higher energy during fracture and exhibit much higher frequency characteristics on their post-peak stage. Additionally, the RA of the same stage is also well correlated to toughness as seen in Fig. 6b. The increase from 17 J to 26 J in toughness is escorted by a decrease of

average RA from 3300 μs/s to 420 μs/V. Both these trends can be reasonably discussed through the fracture mechanisms. Fracture energy is consumed by matrix cracking at the pre-peak stage and mainly by fiber pull-out later. When the bonding between fibers and matrix allows, further matrix cracking continues detaching small volumes of cement matrix that stick with the fibers. As already seen here and in previous studies [26,27], matrix cracking exhibits quite distinct characteristics from fiber pull-out especially concerning RA and AF. The fiber–matrix bonding is enhanced by chemical coating allowing the observation of these simultaneous trends in AE indices and toughness measurements. Another interesting feature comes from the correlation of the average energy of the hits during the pull-out stage with toughness (Fig. 6c). It seems that as the toughness increases by about 50% from the lowest toughness specimen of Fig. 6 to the highest, the average energy of the AE incidents decreases substantially by 95%. This trend implies that specimens with higher toughness suffer many small intensity events compared to specimens with lower mechanical capacity, which rupture by seemingly higher energy events.

This kind of correlations can be generalized for the whole number of concrete mixes studied herein. Stronger correlations emerge with AE indices measured during the post-peak period, when most of the energy is absorbed, rather than the initial micro-cracking stage. Fig. 7a shows the correlation between the average values of AF of the post-peak stage of the six different mixes vs. the average toughness of the specimens of each mix. Each dot is therefore, nominally the average of four values except for the case of rejected specimens (two of the rejected belonged to the treated straight fibers' mix). It is clear that the correlation coefficient R^2, at the post-peak stage is quite strong reaching almost the value of 0.8. As discussed above, higher frequency is connected to matrix cracking rather than pull-out. When fiber pull-out events are escorted with additional matrix cracking due to strong bonding between the fiber and matrix, toughness is reasonable to increase, while the AE frequency characteristics also increase. One noteworthy correlation comes from the total energy recorded by the AE transducers. Fig. 7b shows the total energy of the whole number of AE signals at the post-peak stage vs. the average measured toughness for each concrete mix. It is seen that for mixes with high toughness the cumulative AE energy is decreased. This is reinforced by including the data from specimens without fibers (plain concrete beams) that have been tested with the same experimental setup and their toughness is considered negligible compared to the SFRC. Plain specimens exhibit higher amounts of AE energy throughout their testing. This behavior is connected to the released energy during fracture. For plain material, all energy is released at the instance of macrofracture due to the brittle concrete matrix. However, in the presence of ductile fibers, a substantial part of energy is restrained in the form of plastic deformation. This increases the ab-
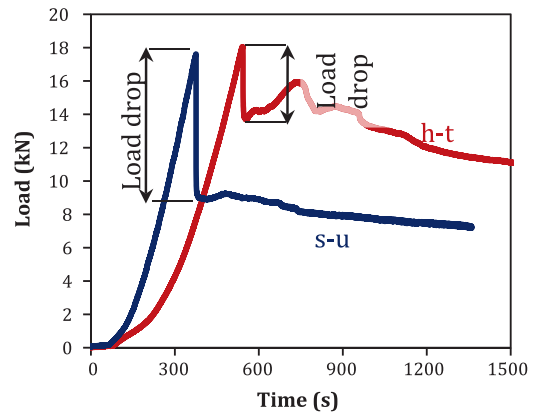

Fig. 8. Load–time histories of SFRC beams (straight-untreated and hooked-treated).

sorbed energy and the finally measured toughness but on the same time decreases the released energy to be recorded by the acoustic emission transducers.

4.2. Load drop

The action of fibers restrains cracking. For plain concrete when the matrix starts to rupture, the crack extends to the top immediately due to the brittleness of concrete and load drops to zero as the material fails destructively. When fibers are present, crack propagation is restrained and the load does not drop to zero, since the material continues to absorb energy, (see Fig. 8) with two typical load–time curves. One is from specimen with hooked and treated fibers and the other from straight and untreated. While they reach approximately the same maximum load, there is a distinct difference at the instantaneous load drop at the instance of major cracking. The specimen with smaller load drop exhibits certainly improved toughness. Thus, the amount of load drop and the deflection increase at the point of fracture may be considered an indication of the ductility of the specimen. The crack is restrained by the action of fibers which are being pulled out while further matrix cracking continues. This increases the volume of the material that absorbs energy decreasing the amount of crack propagation. Chemical coating may further increase the volume of the fracture process zone due to the adhesion that is responsible for detaching a small part of the cement matrix around the fibers. At the instance of load drop the intense cracking phenomena influence the overall toughness, while the amount of load drop and mid span displacement burst correlate again with AE parameters of the signals recorded during macro-fracture (stage II). Fig. 9 shows the correlation between the average value of AF of the six composi-
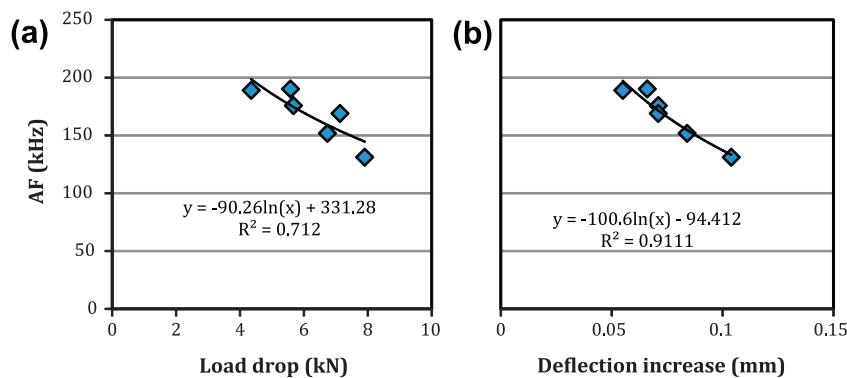

Fig. 9. AF vs. load drop (a) and AF vs. deflection increase (b) at the instance of macro-fracture.

tions of SFRC vs. the load drop at the instance of macro-fracture (a) and vs. the deflection increment that occurs instantly at that point. Again strong correlations are noticed, with specimens that exhibit small load drop and deflection, having higher frequency AE characteristics. As mentioned above this is justified by the extensive matrix cracking that increases the absorbed energy, restrains the crack propagation rate and emits signals with high frequency.

At this point it should be mentioned that the specific values of AE parameters definitely depend on the experimental setup. This includes the type and separation distance of sensors and the specimens' size. Due to material inhomogeneity the acoustic emission signals are distorted and attenuated before being captured by the sensors. Therefore, the specific AE values do not necessarily reflect the waveforms emitted by the tip of the crack. The effect of distance on the values of the AE parameters is discussed by the authors in separate studies [30,31]. The propagation of the crack tip away from the receivers as the deflection increases poses another influence mainly for the matrix cracking signals and less for the pull-out events since fibers are dispersed in the whole volume of the specimen. In the specific case the importance lies on two aspects of the study; first that the experimental setup was fixed for all the tests enabling therefore, comparisons based on the existence or not of the fiber chemical treatment. Second, that parameters measured in a non destructive way exhibited worth-to-mention correlations with the mechanical readings (toughness, load drop etc.) which are always desirable especially in cases in situ where measurements of deflection or load are not possible.

5. Conclusions

This paper describes the acoustic emission behavior of concrete beams with and without chemically treated steel fibers of different shape. Surface treatment of fibers results in strong bonding to the matrix and induces further matrix cracking during fiber pull-out. This leads to distinct acoustic emission behaviors between different concrete mixtures. Specifically, after the main fracture instance, the waveform shape parameter RA remains at high values and average frequency is low for untreated fibers specimens due to the pure friction between fibers and matrix. Treated fibers specimens exhibit an inverse trend concerning these AE indices since fracture includes additional matrix cracking. Analysis of the AE behavior sheds light into the actual active mechanisms during each loading stage. Since the measured mechanical properties and elastic waves emitted during fracture depend on the actual fracture mechanisms, strong correlations emerge between toughness or load parameters and AE descriptors monitored during or after the main crack formation stage. The results imply that independently of the fiber existence, shape or coating, unified correlation curves emerge between fracture toughness and AE parameters like frequency, energy or RA value. This is of paramount importance from the engineering point of view, as it enables the estimation of mechanical performance based on non destructive monitoring.

Acknowledgements

References

[1] Stahli P, van Mier JGM. Manufacturing, fibre anisotropy and fracture of hybrid fibre concrete. Eng Fract Mech 2007;74:223–42.
[2] Pompo A, Stupak PR, Nicolais L, Marchese B. Analysis of steel fibre pull-out from a cement matrix using video photography. Cem Concr Compos 1996;18:3–8.
[3] Shah SP. Do fiber increase the tensile strength of cement-based matrixes. ACI Mater J 1991;88(6):595–602.
[4] Chenkui H, Guofan Z. Properties of steel fibre reinforced concrete containing larger coarse aggregate. Cem Concr Compos 1995;17:199–206.
[5] Soulioti DV, Barkoula NM, Paipetis A, Matikas TE. Effects of fibre geometry and volume fraction on the flexural behaviour of steel–fibre reinforced concrete. Strain 2011;47:e41–e535.
[6] Al-Tayyib AJ, Al-Zahrani M. Use of polypropylene fibres to enhance deterioration resistance of concrete sulfate skin subjected to cyclic wet/dry sea exposure. ACI Mater J 1995;89(4):363–70.
[7] Haddad R, Smadi M. Role of fibres in controlling unrestrained expansion and arresting cracking in Portland cement concrete undergoing alkali–silica reaction. Cem Concr Res 2004;34(1):103–8.
[8] Haddad RH, Abendeh RM. Effect of thermal cycling on bond between reinforcement and fiber reinforced concrete. Cem Concr Compos 2004;26:743–52.
[9] Robins PJ, Austin SA. The resistance of steel fibre concrete to VTOL engine jet blast. Cem Concr Compos 1994;16:57–64.
[10] Chalioris CE, Karayannis CG. Effectiveness of the use of steel fibres on the torsional behavior of flanged concrete beams. Cem Concr Compos 2009;31:331–41.
[11] Kumar A, Gupta AP. Acoustic emission in fibre reinforced concrete. Exp Mech 1996;36(3):258–61.
[12] Pemberton SR, Oberg EK, Dean J, Tsarouchas D, Markaki AE, Marston L, et al. The fracture energy of metal fibre reinforced ceramic composites (MFCs). Compos Sci Technol 2011;71:266–75.
[13] Wu HC, Li VC. Fiber/cement interface tailoring with plasma treatment. Cem Concr Compos 1999;21:205–12.
[14] Sugama T, Carciello N, Kukacka LE. Interface between zinc phosphate deposited steel fibres and cement paste. J Mater Sci 1992;27:2863–72.
[15] Al-mahmoud F, Castel A, Francois R, Tourneur C. Effect of surface preconditioning on bond of carbon fibre reinforced polymer rods to concrete. Cem Concr Compos 2007;29:677–89.
[16] Aggelis DG, Shiotani T, Momoki S, Hirama A. Acoustic emission and ultrasound for damage characterization of concrete elements. ACI Mater J 2009;106(6):509–14.
[17] Chen B, Liu J. Damage in carbon fiber-reinforced concrete, monitored by both electrical resistance measurement and acoustic emission analysis. Construct Build Mater 2008;22:2196–201.
[18] Grosse CU, Ohtsu M. Acoustic emission testing. Heidelberg: Springer; 2008.
[19] Grosse CU, Finck F. Quantitative evaluation of fracture processes in concrete using signal-based acoustic emission techniques. Cem Concr Compos 2006;28:330–6.
[20] Van Tittelboom K, De Belie N, Lehmann F, Grosse CU. Acoustic emission analysis for the quantification of autonomous crack healing in concrete. Construct Build Mater 2012;28:333–41.
[21] Shiotani T. Evaluation of long-term stability for rock slope by means of acoustic emission technique. NDT&E Int 2006;39(3):217–28.
[22] Ohno K, Ohtsu M. Crack classification in concrete based on acoustic emission. Construct Build Mater 2010;24(12):2339–46.
[23] Philippidis TP, Nikolaidis VN, Anastassopoulos AA. Damage characterization of carbon/carbon laminates using neural network techniques on AE signals. NDT&E Int 1998;31(5):329–40.
[24] Aggelis DG, Matikas TE, Shiotani T. Advanced acoustic techniques for health monitoring of concrete structures. In: Kim SH, Ann KY, editors. The Song's handbook of concrete durability. Middleton Publishing Inc.; 2010. p. 331–78.
[25] Aggelis DG, Barkoula NM, Matikas TE, Paipetis AS. Acoustic emission monitoring of degradation of cross ply laminates. J Acoust Soc Am 2010:L246–51.
[26] Soulioti D, Barkoula NM, Paipetis A, Matikas TE, Shiotani T, Aggelis DG. Acoustic emission behavior of steel fibre reinforced concrete under bending. Constr Build Mater 2009;23:3532–6.
[27] Aggelis DG, Soulioti DV, Barkoula NM, Paipetis AS, Matikas TE. Influence of fiber chemical coating on the acoustic emission behavior of steel fiber reinforced concrete. Cem Concr Compos 2012;34:62–7.
[28] Ohtsu M. (Chairman). Recommendations of RILEM Technical Committee 212-ACD: acoustic emission and related NDE techniques for crack detection and damage evaluation in concrete: 3. Test method for classification of active cracks in concrete structures by acoustic emission. Mater Struct 2010; 43(9): 1187-9.
[29] Aggelis DG, Soulioti DV, Sapouridis N, Barkoula NM, Paipetis AS, Matikas TE. Acoustic emission characterization of the fracture process in fibre reinforced concrete. Construct Build Mater 2011;25:4126–31.
[30] Aggelis DG, Mpalaskas AC, Ntalakas D, Matikas TE. Effect of wave distortion on acoustic emission characterization of cementitious materials. Construct Build Mater 2012;35:183–90.
[31] Aggelis DG, Shiotani T, Papacharalampopoulos A, Polyzos D. The influence of propagation path on acoustic emission monitoring of concrete. Struct Health Monitor 2012;11(3):359–66.